Numerical discretization

D.11.1 Discretized function spaces

The exterior problem (D.8) is solved numerically with the boundary element method by employing a Galerkin scheme on the variational formulation of an integral equation. We use on the boundary surface Γ Lagrange finite elements of type either $\mathbb{P}_1$ or $\mathbb{P}_0$. The surface Γ is approximated by the triangular mesh Γ^h, composed by T flat triangles T_j, for $1 \leq j \leq T$, and I nodes $\boldsymbol{r}_i \in \mathbb{R}^3$, $1 \leq i \leq I$. The triangles have a diameter less or equal than h, and their vertices or corners, i.e., the nodes $\boldsymbol{r}_i$, are on top of Γ, as shown in Figure D.5. The diameter of a triangle K is given by

$$\operatorname{diam}(K) = \sup_{\boldsymbol{x},\boldsymbol{y}\in K} |\boldsymbol{y} - \boldsymbol{x}|. \tag{D.188}$$

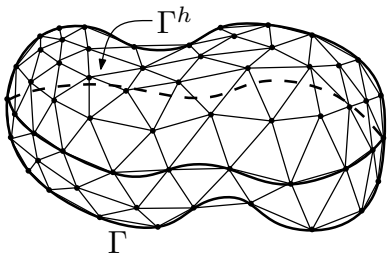

FIGURE D.5. Mesh Γ^h, discretization of Γ.

The function space $H^{1/2}(\Gamma)$ is approximated using the conformal space of continuous piecewise linear polynomials with complex coefficients

$$Q_h = \big\{\varphi_h \in C^0(\Gamma^h) \,:\, \varphi_h|_{T_j} \in \mathbb{P}_1(\mathbb{C}),\;\; 1 \leq j \leq T\big\}. \tag{D.189}$$

The space Q_h has a finite dimension I, and we describe it using the standard base functions for finite elements of type $\mathbb{P}_1$, denoted by $\{\chi_j\}_{j=1}^I$ and illustrated in Figure D.6. The base function χ_j is associated with the node $\boldsymbol{r}_j$ and has its support $\operatorname{supp}\chi_j$ on the triangles that have $\boldsymbol{r}_j$ as one of their vertices. On $\boldsymbol{r}_j$ it has a value of one and on the opposed edges of the triangles its value is zero, being linearly interpolated in between and zero otherwise.

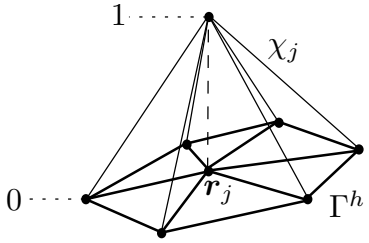

FIGURE D.6. Base function χ_j for finite elements of type $\mathbb{P}_1$.

The function space $H^{-1/2}(\Gamma)$, on the other hand, is approximated using the conformal space of piecewise constant polynomials with complex coefficients

$$P_h = \big\{\psi_h : \Gamma^h \to \mathbb{C} \mid \ \psi_h|_{T_j} \in \mathbb{P}_0(\mathbb{C}), \ \ 1 \le j \le T\big\}. \tag{D.190}$$

The space P_h has a finite dimension T, and is described using the standard base functions for finite elements of type $\mathbb{P}_0$, denoted by $\{\kappa_j\}_{j=1}^T$, shown in Figure D.7, and expressed as

$$\kappa_j(\boldsymbol{x}) = \begin{cases} 1 & \text{if } \ \boldsymbol{x} \in T_j, \\ 0 & \text{if } \ \boldsymbol{x} \notin T_j. \end{cases} \tag{D.191}$$

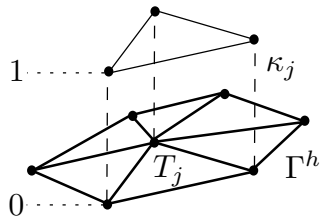

FIGURE D.7. Base function κ_j for finite elements of type $\mathbb{P}_0$.

In virtue of this discretization, any function $\varphi_h \in Q_h$ or $\psi_h \in P_h$ can be expressed as a linear combination of the elements of the base, namely

$$\varphi_h(\boldsymbol{x}) = \sum_{j=1}^{I} \varphi_j \, \chi_j(\boldsymbol{x}) \qquad \text{and} \qquad \psi_h(\boldsymbol{x}) = \sum_{j=1}^{T} \psi_j \, \kappa_j(\boldsymbol{x}) \qquad \text{for } \ \boldsymbol{x} \in \Gamma^h, \tag{D.192}$$

where $\varphi_j, \psi_j \in \mathbb{C}$. The solutions $\mu \in H^{1/2}(\Gamma)$ and $\nu \in H^{-1/2}(\Gamma)$ of the variational formulations can be therefore approximated respectively by

$$\mu_h(\boldsymbol{x}) = \sum_{j=1}^{I} \mu_j \, \chi_j(\boldsymbol{x}) \qquad \text{and} \qquad \nu_h(\boldsymbol{x}) = \sum_{j=1}^{T} \nu_j \, \kappa_j(\boldsymbol{x}) \qquad \text{for } \ \boldsymbol{x} \in \Gamma^h, \tag{D.193}$$

where $\mu_j, \nu_j \in \mathbb{C}$. The function f_z can be also approximated by

$$f_z^h(\boldsymbol{x}) = \sum_{j=1}^{I} f_j \, \chi_j(\boldsymbol{x}) \qquad \text{for } \ \boldsymbol{x} \in \Gamma^h, \quad \text{with } \ f_j = f_z(\boldsymbol{r}_j), \tag{D.194}$$

or

$$f_z^h(\boldsymbol{x}) = \sum_{j=1}^{T} f_j \, \kappa_j(\boldsymbol{x}) \qquad \text{for } \ \boldsymbol{x} \in \Gamma^h, \quad \text{with } \ f_j = \frac{f_z(\boldsymbol{r}_1^j) + f_z(\boldsymbol{r}_2^j) + f_z(\boldsymbol{r}_3^j)}{3}, \tag{D.195}$$

depending on whether the original integral equation is stated in $H^{1/2}(\Gamma)$ or in $H^{-1/2}(\Gamma)$. We denote by $\boldsymbol{r}_d^j$, for $d \in \{1, 2, 3\}$, the three vertices of triangle T_j.

D.11.2 Discretized integral equations

a) First extension by zero

To see how the boundary element method operates, we apply it to the first integral equation of the extension-by-zero alternative, i.e., to the variational formulation (D.183). We characterize all the discrete approximations by the index h, including also the impedance and the boundary layer potentials. The numerical approximation of (D.183) leads to the discretized problem that searches $\mu_h \in Q_h$ such that $\forall \varphi_h \in Q_h$

$$\left\langle \frac{\mu_h}{2} + S_h(Z_h\mu_h) - D_h(\mu_h), \varphi_h \right\rangle = \left\langle S_h(f_z^h), \varphi_h \right\rangle. \tag{D.196}$$

Considering the decomposition of μ_h in terms of the base $\{\chi_j\}$ and taking as test functions the same base functions, $\varphi_h = \chi_i$ for $1 \leq i \leq I$, yields the discrete linear system

$$\sum_{j=1}^{I} \mu_j \left(\frac{1}{2}\langle \chi_j, \chi_i \rangle + \langle S_h(Z_h\chi_j), \chi_i \rangle - \langle D_h(\chi_j), \chi_i \rangle \right) = \sum_{j=1}^{I} f_j \, \langle S_h(\chi_j), \chi_i \rangle. \tag{D.197}$$

This constitutes a system of linear equations that can be expressed as a linear matrix system:

$$\begin{cases} \text{Find } \boldsymbol{\mu} \in \mathbb{C}^I \text{ such that} \\ \boldsymbol{M}\boldsymbol{\mu} = \boldsymbol{b}. \end{cases} \tag{D.198}$$

The elements m_{ij} of the matrix $\boldsymbol{M}$ are given by

$$m_{ij} = \frac{1}{2}\langle \chi_j, \chi_i \rangle + \langle S_h(Z_h\chi_j), \chi_i \rangle - \langle D_h(\chi_j), \chi_i \rangle \qquad \text{for } \; 1 \leq i, j \leq I, \tag{D.199}$$

and the elements b_i of the vector $\boldsymbol{b}$ by

$$b_i = \left\langle S_h(f_z^h), \chi_i \right\rangle = \sum_{j=1}^{I} f_j \, \langle S_h(\chi_j), \chi_i \rangle \qquad \text{for } \; 1 \leq i \leq I. \tag{D.200}$$

The discretized solution u_h, which approximates u, is finally obtained by discretizing the integral representation formula (D.104) according to

$$u_h = \mathcal{D}_h(\mu_h) - \mathcal{S}_h(Z_h\mu_h) + \mathcal{S}_h(f_z^h), \tag{D.201}$$

which, more specifically, can be expressed as

$$u_h = \sum_{j=1}^{I} \mu_j \big(\mathcal{D}_h(\chi_j) - \mathcal{S}_h(Z_h\chi_j) \big) + \sum_{j=1}^{I} f_j \, \mathcal{S}_h(\chi_j). \tag{D.202}$$

By proceeding in the same way, the discretization of all the other alternatives of integral equations can be also expressed as a linear matrix system like (D.198). The resulting matrix $\boldsymbol{M}$ is in general complex, full, non-symmetric, and with dimensions $I \times I$ for elements of type $\mathbb{P}_1$ and $T \times T$ for elements of type $\mathbb{P}_0$. The right-hand side vector $\boldsymbol{b}$ is complex and of size either I or T. The boundary element calculations required to compute numerically the elements of $\boldsymbol{M}$ and $\boldsymbol{b}$ have to be performed carefully, since the integrals that appear become singular when the involved triangles are coincident, or when they have a common vertex or edge, due the singularity of the Green's function at its source point.

b) Second extension by zero

In the case of the second integral equation of the extension-by-zero alternative, i.e., of the variational formulation (D.184), the elements m_{ij} that constitute the matrix $\boldsymbol{M}$ of the linear system (D.198) are given by

$$m_{ij} = \frac{1}{2}\langle Z_h\chi_j, \chi_i\rangle - \langle N_h(\chi_j), \chi_i\rangle + \langle D_h^*(Z_h\chi_j), \chi_i\rangle \qquad \text{for } 1 \le i, j \le I, \tag{D.203}$$

whereas the elements b_i of the vector $\boldsymbol{b}$ are expressed as

$$b_i = \sum_{j=1}^{I} f_j \left(\frac{1}{2}\langle \chi_j, \chi_i\rangle + \langle D_h^*(Z_h\chi_j), \chi_i\rangle\right) \qquad \text{for } 1 \le i \le I. \tag{D.204}$$

The discretized solution u_h is again computed by (D.202).

c) Continuous impedance

In the case of the continuous-impedance alternative, i.e., of the variational formulation (D.185), the elements m_{ij} that constitute the matrix $\boldsymbol{M}$ of the linear system (D.198) are given, for $1 \le i, j \le I$, by

$$m_{ij} = -\langle N_h(\chi_j), \chi_i\rangle + \langle D_h^*(Z_h\chi_j), \chi_i\rangle + \langle Z_h D_h(\chi_j), \chi_i\rangle - \langle Z_h S_h(Z_h\chi_j), \chi_i\rangle, \tag{D.205}$$

whereas the elements b_i of the vector $\boldsymbol{b}$ are expressed as

$$b_i = \sum_{j=1}^{I} f_j \langle \chi_j, \chi_i\rangle \qquad \text{for } 1 \le i \le I. \tag{D.206}$$

It can be observed that for this particular alternative the matrix $\boldsymbol{M}$ turns out to be symmetric, since the integral equation is self-adjoint. The discretized solution u_h, due (D.116), is then computed by

$$u_h = \sum_{j=1}^{I} \mu_j \big(\mathcal{D}_h(\chi_j) - \mathcal{S}_h(Z_h\chi_j)\big). \tag{D.207}$$

d) Continuous value

In the case of the continuous-value alternative, that is, of the variational formulation (D.186), the elements m_{ij} that constitute the matrix $\boldsymbol{M}$, now of the linear system

$$\begin{cases} \text{Find } \boldsymbol{\nu} \in \mathbb{C}^T \text{ such that} \\ \boldsymbol{M\nu} = \boldsymbol{b}, \end{cases} \tag{D.208}$$

are given by

$$m_{ij} = \frac{1}{2}\langle \kappa_j, \kappa_i\rangle + \langle Z_h S_h(\kappa_j), \kappa_i\rangle - \langle D_h^*(\kappa_j), \kappa_i\rangle \qquad \text{for } 1 \le i, j \le T, \tag{D.209}$$

whereas the elements b_i of the vector $\boldsymbol{b}$ are expressed as

$$b_i = -\sum_{j=1}^{T} f_j \langle \kappa_j, \kappa_i\rangle \qquad \text{for } 1 \le i \le T. \tag{D.210}$$

The discretized solution u_h, due (D.124), is then computed by

$$u_h = -\sum_{j=1}^{T} \nu_j \, \mathcal{S}_h(\kappa_j). \tag{D.211}$$

e) Continuous normal derivative

In the case of the continuous-normal-derivative alternative, i.e., of the variational formulation (D.187), the elements m_{ij} that conform the matrix $\boldsymbol{M}$ of the linear system (D.198) are given by

$$m_{ij} = \frac{1}{2}\langle Z_h \chi_j, \chi_i\rangle - \langle N_h(\chi_j), \chi_i\rangle + \langle Z_h D_h(\chi_j), \chi_i\rangle \qquad \text{for } 1 \le i, j \le I, \tag{D.212}$$

whereas the elements b_i of the vector $\boldsymbol{b}$ are expressed as

$$b_i = \sum_{j=1}^{I} f_j \, \langle \chi_j, \chi_i\rangle \qquad \text{for } 1 \le i \le I. \tag{D.213}$$

The discretized solution u_h, due (D.132), is then computed by

$$u_h = \sum_{j=1}^{I} \mu_j \, \mathcal{D}_h(\chi_j). \tag{D.214}$$

D.12 Boundary element calculations

D.12.1 Geometry

The boundary element calculations build the elements of the matrix $\boldsymbol{M}$ resulting from the discretization of the integral equation, i.e., from (D.198) or (D.208). They permit thus to compute numerically expressions like (D.199). To evaluate the appearing singular integrals, we use the semi-numerical methods described in the report of Bendali & Devys (1986).

We consider the elemental interactions between two triangles T_K and T_L of a mesh Γ^h. The unit normal points always inwards of the domain encompassed by the mesh Γ^h.

We denote the triangles more simply just as $K = T_K$ and $L = T_L$. As depicted in Figure D.8, the following notation is used:

- $|K|$ denotes the area of triangle K.
- $|L|$ denotes the area of triangle L.
- $\boldsymbol{r}_1^K, \boldsymbol{r}_2^K, \boldsymbol{r}_3^K$ denote the ordered vertices or corners of triangle K.
- $\boldsymbol{r}_1^L, \boldsymbol{r}_2^L, \boldsymbol{r}_3^L$ denote the ordered vertices or corners of triangle L.
- $\boldsymbol{n}_K, \boldsymbol{n}_L$ denote the unit normals of triangles K and L (oriented with the vertices).

The vertices of the triangles are obtained by renumbering locally the nodes $\boldsymbol{r}_i$, $1 \le i \le I$.

Furthermore, as shown in Figure D.9, we also use the notation:

- h_1^K, h_2^K, h_3^K denote the heights of triangle K.
- h_1^L, h_2^L, h_3^L denote the heights of triangle L.
- $\boldsymbol{\tau}_1^K, \boldsymbol{\tau}_2^K, \boldsymbol{\tau}_3^K$ denote the unit edge tangents of triangle K.

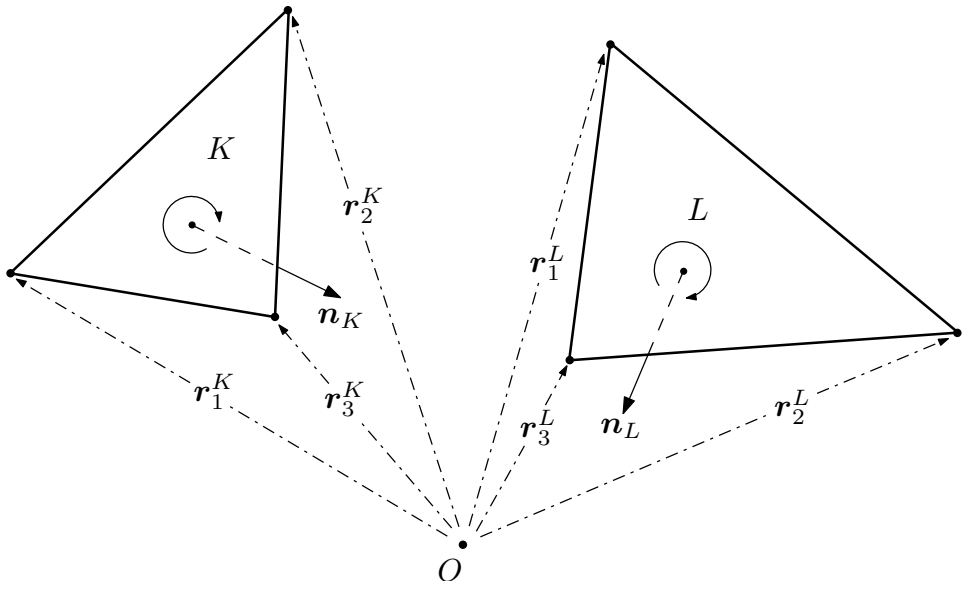

FIGURE D.8. Vertices and unit normals of triangles K and L.

- $\boldsymbol{\tau}_1^L, \boldsymbol{\tau}_2^L, \boldsymbol{\tau}_3^L$ denote the unit edge tangents of triangle L.
- $\boldsymbol{\nu}_1^K, \boldsymbol{\nu}_2^K, \boldsymbol{\nu}_3^K$ denote the unit edge normals of triangle K.
- $\boldsymbol{\nu}_1^L, \boldsymbol{\nu}_2^L, \boldsymbol{\nu}_3^L$ denote the unit edge normals of triangle L.

The unit edge tangents and normals are located on the same plane as the respective triangle.

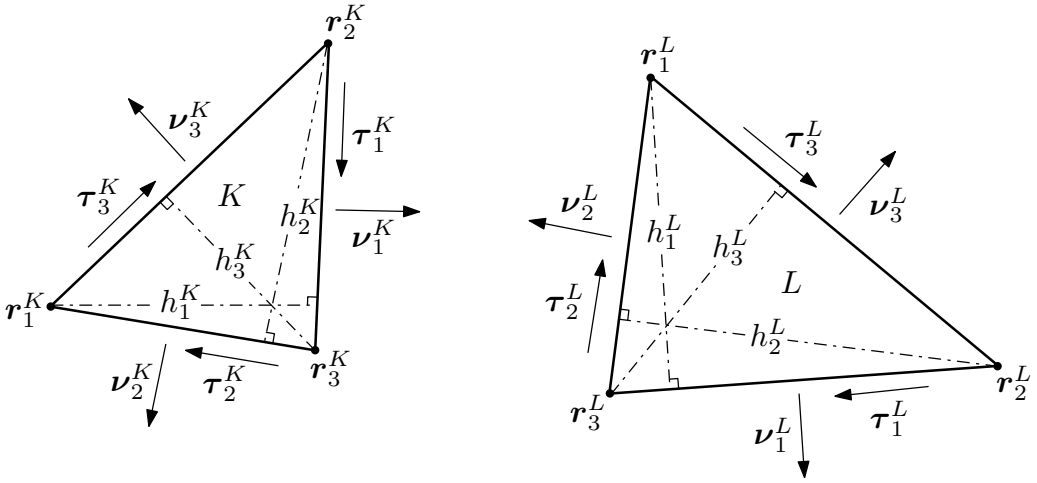

FIGURE D.9. Heights and unit edge normals and tangents of triangles K and L.

For the parametric description of the triangles, shown in Figure D.10, we take into account the notation:

- $\boldsymbol{r}(\boldsymbol{x})$ denotes a variable location on triangle K (dependent on variable $\boldsymbol{x}$).
- $\boldsymbol{r}(\boldsymbol{y})$ denotes a variable location on triangle L (dependent on variable $\boldsymbol{y}$).

- $\boldsymbol{r}_c^K, \boldsymbol{r}_d^L$ denote the vertices of triangles K and L, being $c, d \in \{1, 2, 3\}$.

Triangle K can be parametrically described by

$$\boldsymbol{r}(\boldsymbol{x}) = \boldsymbol{r}_c^K + s_c \boldsymbol{\nu}_c^K + p_c \boldsymbol{\tau}_c^K, \qquad 0 \leq s_c \leq h_c^K, \qquad c \in \{1, 2, 3\}, \tag{D.215}$$

where

$$-\frac{s_1}{h_1^K}(\boldsymbol{r}_1^K - \boldsymbol{r}_2^K) \cdot \boldsymbol{\tau}_1^K \leq p_1 \leq \frac{s_1}{h_1^K}(\boldsymbol{r}_3^K - \boldsymbol{r}_1^K) \cdot \boldsymbol{\tau}_1^K, \tag{D.216}$$

$$-\frac{s_2}{h_2^K}(\boldsymbol{r}_2^K - \boldsymbol{r}_3^K) \cdot \boldsymbol{\tau}_2^K \leq p_2 \leq \frac{s_2}{h_2^K}(\boldsymbol{r}_1^K - \boldsymbol{r}_2^K) \cdot \boldsymbol{\tau}_2^K, \tag{D.217}$$

$$-\frac{s_3}{h_3^K}(\boldsymbol{r}_3^K - \boldsymbol{r}_1^K) \cdot \boldsymbol{\tau}_3^K \leq p_3 \leq \frac{s_3}{h_3^K}(\boldsymbol{r}_2^K - \boldsymbol{r}_3^K) \cdot \boldsymbol{\tau}_3^K. \tag{D.218}$$

Similarly, triangle L can be parametrically described by

$$\boldsymbol{r}(\boldsymbol{y}) = \boldsymbol{r}_d^L + t_d \boldsymbol{\nu}_d^L + q_d \boldsymbol{\tau}_d^L, \qquad 0 \leq t_d \leq h_d^L, \qquad d \in \{1, 2, 3\}, \tag{D.219}$$

where

$$-\frac{t_1}{h_1^L}(\boldsymbol{r}_1^L - \boldsymbol{r}_2^L) \cdot \boldsymbol{\tau}_1^L \leq q_1 \leq \frac{t_1}{h_1^L}(\boldsymbol{r}_3^L - \boldsymbol{r}_1^L) \cdot \boldsymbol{\tau}_1^L, \tag{D.220}$$

$$-\frac{t_2}{h_2^L}(\boldsymbol{r}_2^L - \boldsymbol{r}_3^L) \cdot \boldsymbol{\tau}_2^L \leq q_2 \leq \frac{t_2}{h_2^L}(\boldsymbol{r}_1^L - \boldsymbol{r}_2^L) \cdot \boldsymbol{\tau}_2^L, \tag{D.221}$$

$$-\frac{t_3}{h_3^L}(\boldsymbol{r}_3^L - \boldsymbol{r}_1^L) \cdot \boldsymbol{\tau}_3^L \leq q_3 \leq \frac{t_3}{h_3^L}(\boldsymbol{r}_2^L - \boldsymbol{r}_3^L) \cdot \boldsymbol{\tau}_3^L. \tag{D.222}$$

Thus the parameters p_c, s_c, q_d, and t_d can be expressed as

$$p_c = \big(\boldsymbol{r}(\boldsymbol{x}) - \boldsymbol{r}_c^K\big) \cdot \boldsymbol{\tau}_c^K, \qquad c \in \{1, 2, 3\}, \tag{D.223}$$

$$s_c = \big(\boldsymbol{r}(\boldsymbol{x}) - \boldsymbol{r}_c^K\big) \cdot \boldsymbol{\nu}_c^K, \qquad c \in \{1, 2, 3\}, \tag{D.224}$$

$$q_d = \big(\boldsymbol{r}(\boldsymbol{y}) - \boldsymbol{r}_d^L\big) \cdot \boldsymbol{\tau}_d^L, \qquad d \in \{1, 2, 3\}. \tag{D.225}$$

$$t_d = \big(\boldsymbol{r}(\boldsymbol{y}) - \boldsymbol{r}_d^L\big) \cdot \boldsymbol{\nu}_d^L, \qquad d \in \{1, 2, 3\}. \tag{D.226}$$

The areas of the triangles K and L are given by

$$|K| = \frac{1}{2} h_1^K |\boldsymbol{r}_3^K - \boldsymbol{r}_2^K| = \frac{1}{2} h_2^K |\boldsymbol{r}_3^K - \boldsymbol{r}_1^K| = \frac{1}{2} h_3^K |\boldsymbol{r}_2^K - \boldsymbol{r}_1^K|, \tag{D.227}$$

$$|L| = \frac{1}{2} h_1^L |\boldsymbol{r}_3^L - \boldsymbol{r}_2^L| = \frac{1}{2} h_2^L |\boldsymbol{r}_3^L - \boldsymbol{r}_1^L| = \frac{1}{2} h_3^L |\boldsymbol{r}_2^L - \boldsymbol{r}_1^L|. \tag{D.228}$$

The unit normals $\boldsymbol{n}_K$ and $\boldsymbol{n}_L$ can be computed as

$$\boldsymbol{n}_K = \frac{\boldsymbol{\tau}_1^K \times \boldsymbol{\tau}_2^K}{|\boldsymbol{\tau}_1^K \times \boldsymbol{\tau}_2^K|} = \frac{\boldsymbol{\tau}_2^K \times \boldsymbol{\tau}_3^K}{|\boldsymbol{\tau}_2^K \times \boldsymbol{\tau}_3^K|} = \frac{\boldsymbol{\tau}_3^K \times \boldsymbol{\tau}_1^K}{|\boldsymbol{\tau}_3^K \times \boldsymbol{\tau}_1^K|}, \tag{D.229}$$

$$\boldsymbol{n}_L = \frac{\boldsymbol{\tau}_1^L \times \boldsymbol{\tau}_2^L}{|\boldsymbol{\tau}_1^L \times \boldsymbol{\tau}_2^L|} = \frac{\boldsymbol{\tau}_2^L \times \boldsymbol{\tau}_3^L}{|\boldsymbol{\tau}_2^L \times \boldsymbol{\tau}_3^L|} = \frac{\boldsymbol{\tau}_3^L \times \boldsymbol{\tau}_1^L}{|\boldsymbol{\tau}_3^L \times \boldsymbol{\tau}_1^L|}. \tag{D.230}$$

For the unit edge tangents $\boldsymbol{\tau}_c^K$ and $\boldsymbol{\tau}_d^L$ we have that

$$\boldsymbol{\tau}_1^K = \frac{\boldsymbol{r}_3^K - \boldsymbol{r}_2^K}{|\boldsymbol{r}_3^K - \boldsymbol{r}_2^K|}, \qquad \boldsymbol{\tau}_2^K = \frac{\boldsymbol{r}_1^K - \boldsymbol{r}_3^K}{|\boldsymbol{r}_1^K - \boldsymbol{r}_3^K|}, \qquad \boldsymbol{\tau}_3^K = \frac{\boldsymbol{r}_2^K - \boldsymbol{r}_1^K}{|\boldsymbol{r}_2^K - \boldsymbol{r}_1^K|}, \tag{D.231}$$

$$\boldsymbol{\tau}_1^L = \frac{\boldsymbol{r}_3^L - \boldsymbol{r}_2^L}{|\boldsymbol{r}_3^L - \boldsymbol{r}_2^L|}, \qquad \boldsymbol{\tau}_2^L = \frac{\boldsymbol{r}_1^L - \boldsymbol{r}_3^L}{|\boldsymbol{r}_1^L - \boldsymbol{r}_3^L|}, \qquad \boldsymbol{\tau}_3^L = \frac{\boldsymbol{r}_2^L - \boldsymbol{r}_1^L}{|\boldsymbol{r}_2^L - \boldsymbol{r}_1^L|}, \tag{D.232}$$

and for the unit edge normals $\boldsymbol{\nu}_c^K$ and $\boldsymbol{\nu}_d^L$, that

$$\boldsymbol{\nu}_c^K = \boldsymbol{\tau}_c^K \times \boldsymbol{n}_K, \qquad c \in \{1,2,3\}, \tag{D.233}$$

$$\boldsymbol{\nu}_d^L = \boldsymbol{\tau}_d^L \times \boldsymbol{n}_L, \qquad d \in \{1,2,3\}. \tag{D.234}$$

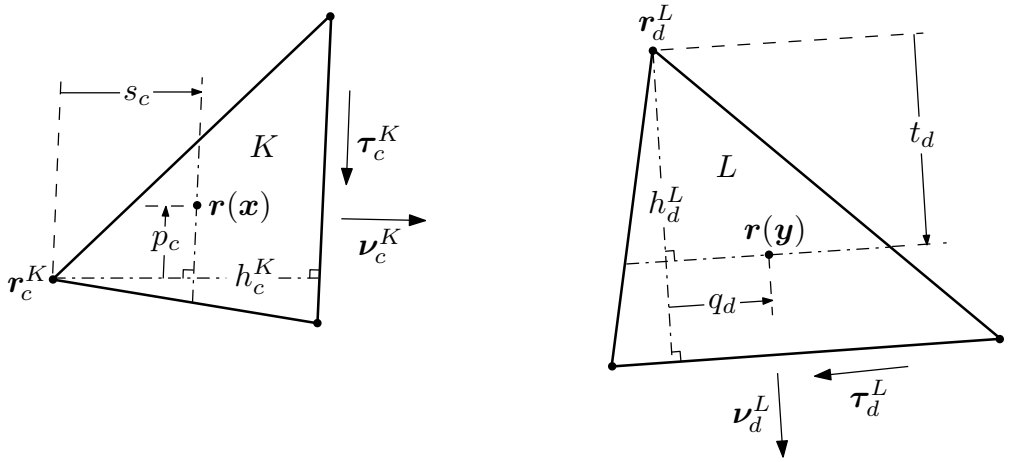

FIGURE D.10. Parametric description of triangles K and L.

The triangles K and L can be also parametrically described using barycentric coordinates λ_c^K and λ_d^L, i.e.,

$$\boldsymbol{r}(\boldsymbol{x}) = \sum_{c=1}^{3} \lambda_c^K \boldsymbol{r}_c^K, \qquad \sum_{c=1}^{3} \lambda_c^K = 1, \qquad 0 \leq \lambda_c^K \leq 1, \tag{D.235}$$

$$\boldsymbol{r}(\boldsymbol{y}) = \sum_{d=1}^{3} \lambda_d^L \boldsymbol{r}_d^L, \qquad \sum_{d=1}^{3} \lambda_d^L = 1, \qquad 0 \leq \lambda_d^L \leq 1. \tag{D.236}$$

For the elemental interactions between a point $\boldsymbol{x}$ on triangle K and a point $\boldsymbol{y}$ on triangle L, the following notation is also used:

- $\boldsymbol{R}$ denotes the vector pointing from the point $\boldsymbol{x}$ towards the point $\boldsymbol{y}$.
- R denotes the distance between the points $\boldsymbol{x}$ and $\boldsymbol{y}$.

These values are given by

$$\boldsymbol{R} = \boldsymbol{r}(\boldsymbol{y}) - \boldsymbol{r}(\boldsymbol{x}), \tag{D.237}$$

$$R = |\boldsymbol{R}| = |\boldsymbol{y} - \boldsymbol{x}|. \tag{D.238}$$

For the singular integral calculations, when considering the point $\boldsymbol{x}$ as a parameter, the following notation is also used (vid. Figure D.11):

- $\boldsymbol{R}_1^L, \boldsymbol{R}_2^L, \boldsymbol{R}_3^L$ denote the vectors pointing from $\boldsymbol{x}$ towards the vertices of triangle L.

- R_1^L, R_2^L, R_3^L denote the distances from $\boldsymbol{x}$ to the vertices of triangle L.
- C_1^L, C_2^L, C_3^L denote the edges or sides of triangle L.
- d_L denotes the signed distance from $\boldsymbol{x}$ to the plane that contains triangle L.
- Θ_L denotes the solid angle formed by the vectors $\boldsymbol{R}_1^L$, $\boldsymbol{R}_2^L$, and $\boldsymbol{R}_3^L$, through which triangle L is seen from point $\boldsymbol{x}$ ($-2\pi \leq \Theta_L \leq 2\pi$).

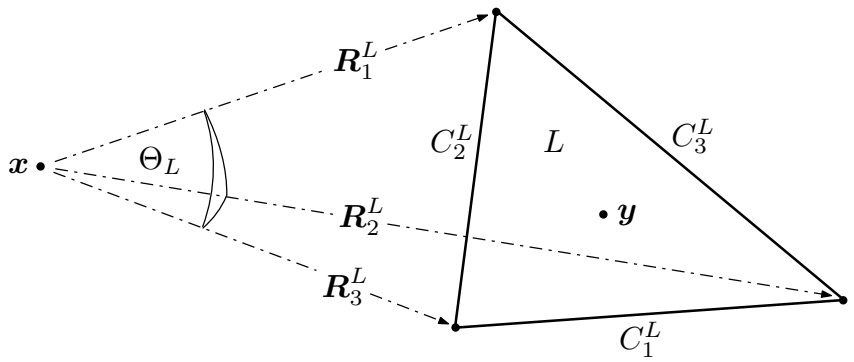

FIGURE D.11. Geometric characteristics for the singular integral calculations.

Thus on triangle L the following holds:

$$\boldsymbol{R}_d^L = \boldsymbol{r}_d^L - \boldsymbol{r}(\boldsymbol{x}), \qquad R_d^L = |\boldsymbol{R}_d^L|, \qquad d \in \{1,2,3\}. \tag{D.239}$$

Likewise as before, we have for $d \in \{1,2,3\}$ that

$$\boldsymbol{R} = \boldsymbol{R}_d^L + t_d\, \boldsymbol{\nu}_d^L + q_d\, \boldsymbol{\tau}_d^L, \tag{D.240}$$

$$t_d = \big(\boldsymbol{R} - \boldsymbol{R}_d^L\big) \cdot \boldsymbol{\nu}_d^L, \tag{D.241}$$

$$q_d = \big(\boldsymbol{R} - \boldsymbol{R}_d^L\big) \cdot \boldsymbol{\tau}_d^L. \tag{D.242}$$

In particular, the edges C_d^L are parametrically described by

$$\boldsymbol{R} = \boldsymbol{R}_d^L + h_d^L\, \boldsymbol{\nu}_d^L + q_d\, \boldsymbol{\tau}_d^L. \tag{D.243}$$

The signed distance d_L is constant on L and is characterized by

$$d_L = \boldsymbol{R} \cdot \boldsymbol{n}_L = \boldsymbol{R}_1^L \cdot \boldsymbol{n}_L = \boldsymbol{R}_2^L \cdot \boldsymbol{n}_L = \boldsymbol{R}_3^L \cdot \boldsymbol{n}_L. \tag{D.244}$$

Finally, the solid angle Θ_L can be computed by using the formula described in the article of Van Oosterom & Strackee (1983):

$$\tan\left(\frac{\Theta_L}{2}\right) = \frac{\big[\boldsymbol{R}_1^L \boldsymbol{R}_2^L \boldsymbol{R}_3^L\big]}{R_1^L R_2^L R_3^L + (\boldsymbol{R}_1^L \cdot \boldsymbol{R}_2^L) R_3^L + (\boldsymbol{R}_1^L \cdot \boldsymbol{R}_3^L) R_2^L + (\boldsymbol{R}_2^L \cdot \boldsymbol{R}_3^L) R_1^L}, \tag{D.245}$$

where $-2\pi \leq \Theta_L \leq 2\pi$ and where the triple scalar product

$$\big[\boldsymbol{R}_1^L \boldsymbol{R}_2^L \boldsymbol{R}_3^L\big] = \boldsymbol{R}_1^L \cdot (\boldsymbol{R}_2^L \times \boldsymbol{R}_3^L) = \boldsymbol{R}_2^L \cdot (\boldsymbol{R}_3^L \times \boldsymbol{R}_1^L) = \boldsymbol{R}_3^L \cdot (\boldsymbol{R}_1^L \times \boldsymbol{R}_2^L) \tag{D.246}$$

represents the signed volume of the parallelepiped spanned by the vectors $\boldsymbol{R}_1^L$, $\boldsymbol{R}_2^L$, and $\boldsymbol{R}_3^L$.

D.12.2 Boundary element integrals

The boundary element integrals are the basic integrals needed to perform the boundary element calculations. In our case, by considering $a, b \in \{0, 1\}$ and $c, d \in \{1, 2, 3\}$, they can be expressed as

$$ZA_{a,b}^{c,d} = \int_K \int_L \left(\frac{s_c}{h_c^K}\right)^a \left(\frac{t_d}{h_d^L}\right)^b G(\boldsymbol{x}, \boldsymbol{y}) \, \mathrm{d}L(\boldsymbol{y}) \, \mathrm{d}K(\boldsymbol{x}), \tag{D.247}$$

$$ZB_{a,b}^{c,d} = \int_K \int_L \left(\frac{s_c}{h_c^K}\right)^a \left(\frac{t_d}{h_d^L}\right)^b \frac{\partial G}{\partial n_{\boldsymbol{y}}}(\boldsymbol{x}, \boldsymbol{y}) \, \mathrm{d}L(\boldsymbol{y}) \, \mathrm{d}K(\boldsymbol{x}), \tag{D.248}$$

$$ZC_{a,b}^{c,d} = \int_K \int_L \left(\frac{s_c}{h_c^K}\right)^a \left(\frac{t_d}{h_d^L}\right)^b \frac{\partial G}{\partial n_{\boldsymbol{x}}}(\boldsymbol{x}, \boldsymbol{y}) \, \mathrm{d}L(\boldsymbol{y}) \, \mathrm{d}K(\boldsymbol{x}), \tag{D.249}$$

where the parameters s_c and t_d depend respectively on the variables $\boldsymbol{x}$ and $\boldsymbol{y}$, as stated in (D.224) and (D.226). When the triangles have to be specified, i.e., if $K = T_i$ and $L = T_j$, then we state it respectively as $ZA_{a,b}^{c,d}(T_i, T_j)$, $ZB_{a,b}^{c,d}(T_i, T_j)$, or $ZC_{a,b}^{c,d}(T_i, T_j)$, e.g.,

$$ZA_{a,b}^{c,d}(T_i, T_j) = \int_{T_i} \int_{T_j} \left(\frac{s_c}{h_c^K}\right)^a \left(\frac{t_d}{h_d^L}\right)^b G(\boldsymbol{x}, \boldsymbol{y}) \, \mathrm{d}\gamma(\boldsymbol{y}) \, \mathrm{d}\gamma(\boldsymbol{x}). \tag{D.250}$$

It should be observed that (D.249) can be expressed in terms of (D.248):

$$ZC_{a,b}^{c,d}(T_i, T_j) = ZB_{b,a}^{d,c}(T_j, T_i), \tag{D.251}$$

since the involved operators are self-adjoint. It occurs therefore that all the integrals that stem from the numerical discretization can be expressed in terms of the two basic boundary element integrals (D.247) and (D.248).

For this to hold true, the impedance is discretized as a piecewise constant function Z_h, which on each triangle T_j adopts a constant value $Z_j \in \mathbb{C}$, e.g.,

$$Z_h|_{T_j} = Z_j = \frac{1}{3}\Big(Z\big(\boldsymbol{r}_1^{T_j}\big) + Z\big(\boldsymbol{r}_2^{T_j}\big) + Z\big(\boldsymbol{r}_3^{T_j}\big)\Big). \tag{D.252}$$

Now we can compute all the integrals of interest. We begin with the ones that are related with the finite elements of type $\mathbb{P}_0$, which are easier. It can be observed that

$$\langle \kappa_j, \kappa_i \rangle = \int_{\Gamma^h} \kappa_j(\boldsymbol{x}) \kappa_i(\boldsymbol{x}) \, \mathrm{d}\gamma(\boldsymbol{x}) = \begin{cases} |T_i| & \text{if } j = i, \\ 0 & \text{if } j \neq i. \end{cases} \tag{D.253}$$

We have likewise that

$$\begin{aligned} \langle Z_h S_h(\kappa_j), \kappa_i \rangle &= \int_{\Gamma^h} \int_{\Gamma^h} Z_h(\boldsymbol{x}) G(\boldsymbol{x}, \boldsymbol{y}) \kappa_j(\boldsymbol{y}) \kappa_i(\boldsymbol{x}) \, \mathrm{d}\gamma(\boldsymbol{y}) \, \mathrm{d}\gamma(\boldsymbol{x}) \\ &= Z_i ZA_{0,0}^{c,d}(T_i, T_j), \end{aligned} \tag{D.254}$$

which is independent of $c, d \in \{1, 2, 3\}$. It holds similarly that

$$\langle D_h^*(\kappa_j), \kappa_i \rangle = \int_{\Gamma^h} \int_{\Gamma^h} \frac{\partial G}{\partial n_{\boldsymbol{x}}}(\boldsymbol{x}, \boldsymbol{y}) \kappa_j(\boldsymbol{y}) \kappa_i(\boldsymbol{x}) \, \mathrm{d}\gamma(\boldsymbol{y}) \, \mathrm{d}\gamma(\boldsymbol{x}) = ZB_{0,0}^{d,c}(T_j, T_i), \tag{D.255}$$

which is again independent of $c, d \in \{1, 2, 3\}$. We consider now the integrals for the finite elements of type $\mathbb{P}_1$. By taking as zero the sum over an empty set, we have that

$$\langle \chi_j, \chi_i \rangle = \int_{\Gamma^h} \chi_j(\boldsymbol{x}) \chi_i(\boldsymbol{x}) \, \mathrm{d}\gamma(\boldsymbol{x}) = \begin{cases} \displaystyle\sum_{K \ni \boldsymbol{r}_i} \frac{|K|}{6} & \text{if } \ j = i, \\ \displaystyle\sum_{K \ni \boldsymbol{r}_i, \boldsymbol{r}_j} \frac{|K|}{12} & \text{if } \ i \neq j. \end{cases} \tag{D.256}$$

In the same way, it occurs that

$$\langle Z_h \chi_j, \chi_i \rangle = \begin{cases} \displaystyle\sum_{K \ni \boldsymbol{r}_i} \frac{Z_K |K|}{6} & \text{if } \ j = i, \\ \displaystyle\sum_{K \ni \boldsymbol{r}_i, \boldsymbol{r}_j} \frac{Z_K |K|}{12} & \text{if } \ i \neq j. \end{cases} \tag{D.257}$$

We have also that

$$\begin{aligned} \langle S_h(\chi_j), \chi_i \rangle &= \int_{\Gamma^h} \int_{\Gamma^h} G(\boldsymbol{x}, \boldsymbol{y}) \chi_j(\boldsymbol{y}) \chi_i(\boldsymbol{x}) \, \mathrm{d}\gamma(\boldsymbol{y}) \, \mathrm{d}\gamma(\boldsymbol{x}) \\ &= \sum_{K \ni \boldsymbol{r}_i} \sum_{L \ni \boldsymbol{r}_j} \left(ZA_{0,0}^{c_i^K, d_j^L} - ZA_{0,1}^{c_i^K, d_j^L} - ZA_{1,0}^{c_i^K, d_j^L} + ZA_{1,1}^{c_i^K, d_j^L} \right), \end{aligned} \tag{D.258}$$

where the local subindexes c_i^K and d_j^L are always such that

$$\boldsymbol{r}_{c_i^K}^K = \boldsymbol{r}_i \qquad \text{and} \qquad \boldsymbol{r}_{d_j^L}^L = \boldsymbol{r}_j, \tag{D.259}$$

and where we use the more simplified notation

$$ZA_{a,b}^{c_i^K, d_j^L} = ZA_{a,b}^{c_i^K, d_j^L}(K, L). \tag{D.260}$$

Additionally it holds that

$$\begin{aligned} \langle S_h(Z_h \chi_j), \chi_i \rangle &= \int_{\Gamma^h} \int_{\Gamma^h} Z_h(\boldsymbol{y}) G(\boldsymbol{x}, \boldsymbol{y}) \chi_j(\boldsymbol{y}) \chi_i(\boldsymbol{x}) \, \mathrm{d}\gamma(\boldsymbol{y}) \, \mathrm{d}\gamma(\boldsymbol{x}) \\ &= \sum_{K \ni \boldsymbol{r}_i} \sum_{L \ni \boldsymbol{r}_j} Z_L \left(ZA_{0,0}^{c_i^K, d_j^L} - ZA_{0,1}^{c_i^K, d_j^L} - ZA_{1,0}^{c_i^K, d_j^L} + ZA_{1,1}^{c_i^K, d_j^L} \right). \end{aligned} \tag{D.261}$$

Furthermore we see that

$$\begin{aligned} \langle Z_h S_h(Z_h \chi_j), \chi_i \rangle &= \int_{\Gamma^h} \int_{\Gamma^h} Z_h(\boldsymbol{x}) Z_h(\boldsymbol{y}) G(\boldsymbol{x}, \boldsymbol{y}) \chi_j(\boldsymbol{y}) \chi_i(\boldsymbol{x}) \, \mathrm{d}\gamma(\boldsymbol{y}) \, \mathrm{d}\gamma(\boldsymbol{x}) \\ &= \sum_{K \ni \boldsymbol{r}_i} \sum_{L \ni \boldsymbol{r}_j} Z_K Z_L \left(ZA_{0,0}^{c_i^K, d_j^L} - ZA_{0,1}^{c_i^K, d_j^L} - ZA_{1,0}^{c_i^K, d_j^L} + ZA_{1,1}^{c_i^K, d_j^L} \right). \end{aligned} \tag{D.262}$$

Likewise it occurs that

$$\begin{aligned} \langle D_h(\chi_j), \chi_i \rangle &= \int_{\Gamma^h} \int_{\Gamma^h} \frac{\partial G}{\partial n_{\boldsymbol{y}}}(\boldsymbol{x}, \boldsymbol{y}) \chi_j(\boldsymbol{y}) \chi_i(\boldsymbol{x}) \, \mathrm{d}\gamma(\boldsymbol{y}) \, \mathrm{d}\gamma(\boldsymbol{x}) \\ &= \sum_{K \ni \boldsymbol{r}_i} \sum_{L \ni \boldsymbol{r}_j} \left(ZB_{0,0}^{c_i^K, d_j^L} - ZB_{0,1}^{c_i^K, d_j^L} - ZB_{1,0}^{c_i^K, d_j^L} + ZB_{1,1}^{c_i^K, d_j^L} \right). \end{aligned} \tag{D.263}$$

It holds moreover that

$$\langle Z_h D_h(\chi_j), \chi_i \rangle = \int_{\Gamma^h} \int_{\Gamma^h} Z_h(\boldsymbol{x}) \frac{\partial G}{\partial n_{\boldsymbol{y}}}(\boldsymbol{x}, \boldsymbol{y}) \chi_j(\boldsymbol{y}) \chi_i(\boldsymbol{x}) \, \mathrm{d}\gamma(\boldsymbol{y}) \, \mathrm{d}\gamma(\boldsymbol{x})$$
$$= \sum_{K \ni \boldsymbol{r}_i} \sum_{L \ni \boldsymbol{r}_j} Z_K \left(ZB_{0,0}^{c_i^K, d_j^L} - ZB_{0,1}^{c_i^K, d_j^L} - ZB_{1,0}^{c_i^K, d_j^L} + ZB_{1,1}^{c_i^K, d_j^L} \right). \quad \text{(D.264)}$$

We have also that

$$\langle D_h^*(\chi_j), \chi_i \rangle = \int_{\Gamma^h} \int_{\Gamma^h} \frac{\partial G}{\partial n_{\boldsymbol{x}}}(\boldsymbol{x}, \boldsymbol{y}) \chi_j(\boldsymbol{y}) \chi_i(\boldsymbol{x}) \, \mathrm{d}\gamma(\boldsymbol{y}) \, \mathrm{d}\gamma(\boldsymbol{x})$$
$$= \sum_{K \ni \boldsymbol{r}_i} \sum_{L \ni \boldsymbol{r}_j} \left(ZB_{0,0}^{d_j^L, c_i^K} - ZB_{1,0}^{d_j^L, c_i^K} - ZB_{0,1}^{d_j^L, c_i^K} + ZB_{1,1}^{d_j^L, c_i^K} \right), \quad \text{(D.265)}$$

where the change in index order is understood as

$$ZB_{b,a}^{d_j^L, c_i^K} = ZB_{b,a}^{d_j^L, c_i^K}(L, K). \quad \text{(D.266)}$$

Similarly it occurs that

$$\langle D_h^*(Z_h \chi_j), \chi_i \rangle = \int_{\Gamma^h} \int_{\Gamma^h} Z_h(\boldsymbol{y}) \frac{\partial G}{\partial n_{\boldsymbol{x}}}(\boldsymbol{x}, \boldsymbol{y}) \chi_j(\boldsymbol{y}) \chi_i(\boldsymbol{x}) \, \mathrm{d}\gamma(\boldsymbol{y}) \, \mathrm{d}\gamma(\boldsymbol{x})$$
$$= \sum_{K \ni \boldsymbol{r}_i} \sum_{L \ni \boldsymbol{r}_j} Z_L \left(ZB_{0,0}^{d_j^L, c_i^K} - ZB_{1,0}^{d_j^L, c_i^K} - ZB_{0,1}^{d_j^L, c_i^K} + ZB_{1,1}^{d_j^L, c_i^K} \right). \quad \text{(D.267)}$$

And finally, for the hypersingular term we have that

$$\langle N_h(\chi_j), \chi_i \rangle = - \int_{\Gamma^h} \int_{\Gamma^h} G(\boldsymbol{x}, \boldsymbol{y}) \big(\nabla \chi_j(\boldsymbol{y}) \times \boldsymbol{n}_{\boldsymbol{y}} \big) \cdot \big(\nabla \chi_i(\boldsymbol{x}) \times \boldsymbol{n}_{\boldsymbol{x}} \big) \, \mathrm{d}\gamma(\boldsymbol{y}) \, \mathrm{d}\gamma(\boldsymbol{x})$$
$$= - \sum_{K \ni \boldsymbol{r}_i} \sum_{L \ni \boldsymbol{r}_j} \frac{ZA_{0,0}^{c_i^K, d_j^L}}{h_{c_i^K}^K h_{d_j^L}^L} \big(\boldsymbol{\nu}_{c_i^K}^K \times \boldsymbol{n}_K \big) \cdot \big(\boldsymbol{\nu}_{d_j^L}^L \times \boldsymbol{n}_L \big). \quad \text{(D.268)}$$

It remains now to compute the integrals (D.247) and (D.248), which are calculated in two steps with a semi-numerical integration, i.e., the singular parts are calculated analytically and the other parts numerically. First the internal integral for $\boldsymbol{y}$ is computed, then the external one for $\boldsymbol{x}$. This can be expressed as

$$ZA_{a,b}^{c,d} = \int_K \left(\frac{s_c}{h_c^K} \right)^a ZF_b^d(\boldsymbol{x}) \, \mathrm{d}K(\boldsymbol{x}), \quad \text{(D.269)}$$

$$ZF_b^d(\boldsymbol{x}) = \int_L \left(\frac{t_d}{h_d^L} \right)^b G(\boldsymbol{x}, \boldsymbol{y}) \, \mathrm{d}L(\boldsymbol{y}), \quad \text{(D.270)}$$

and

$$ZB_{a,b}^{c,d} = \int_K \left(\frac{s_c}{h_c^K} \right)^a ZG_b^d(\boldsymbol{x}) \, \mathrm{d}K(\boldsymbol{x}), \quad \text{(D.271)}$$

$$ZG_b^d(\boldsymbol{x}) = \int_L \left(\frac{t_d}{h_d^L} \right)^b \frac{\partial G}{\partial n_{\boldsymbol{y}}}(\boldsymbol{x}, \boldsymbol{y}) \, \mathrm{d}L(\boldsymbol{y}). \quad \text{(D.272)}$$

This kind of integrals can be also used to compute the terms associated with the discretized solution u_h. Using an analogous notation as in (D.250), we have that

$$\mathcal{S}_h(\kappa_j) = \int_{\Gamma^h} G(\boldsymbol{x},\boldsymbol{y})\kappa_j(\boldsymbol{y})\,\mathrm{d}\gamma(\boldsymbol{y}) = ZF_0^d(T_j)(\boldsymbol{x}), \tag{D.273}$$

which is independent of $d \in \{1,2,3\}$. Similarly it holds that

$$\mathcal{S}_h(\chi_j) = \int_{\Gamma^h} G(\boldsymbol{x},\boldsymbol{y})\chi_j(\boldsymbol{y})\,\mathrm{d}\gamma(\boldsymbol{y}) = \sum_{L\ni\boldsymbol{r}_j}\left(ZF_0^{d_j^L}(L)(\boldsymbol{x}) - ZF_1^{d_j^L}(L)(\boldsymbol{x})\right), \tag{D.274}$$

and

$$\mathcal{S}_h(Z_h\chi_j) = \int_{\Gamma^h} Z_h(\boldsymbol{y})G(\boldsymbol{x},\boldsymbol{y})\chi_j(\boldsymbol{y})\,\mathrm{d}\gamma(\boldsymbol{y}) = \sum_{L\ni\boldsymbol{r}_j} Z_L\left(ZF_0^{d_j^L}(L)(\boldsymbol{x}) - ZF_1^{d_j^L}(L)(\boldsymbol{x})\right). \tag{D.275}$$

The remaining term is computed as

$$\mathcal{D}_h(\chi_j) = \int_{\Gamma^h} \frac{\partial G}{\partial n_{\boldsymbol{y}}}(\boldsymbol{x},\boldsymbol{y})\chi_j(\boldsymbol{y})\,\mathrm{d}\gamma(\boldsymbol{y}) = \sum_{L\ni\boldsymbol{r}_j}\left(ZG_0^{d_j^L}(L)(\boldsymbol{x}) - ZG_1^{d_j^L}(L)(\boldsymbol{x})\right). \tag{D.276}$$

D.12.3 Numerical integration for the non-singular integrals

For the numerical integration of the non-singular integrals of the boundary element calculations we use three-point and six-point Gauss-Lobatto quadrature formulae (cf., e.g. Cowper 1973, Dunavant 1985). We describe the triangles K and L by means of barycentric coordinates as done in (D.235) and (D.236).

a) Three-point Gauss-Lobatto quadrature formulae

As shown in Figure D.12, for the three-point Gauss-Lobatto quadrature we consider, respectively on the triangles K and L, the points

$$\boldsymbol{x}_1 = \frac{2}{3}\boldsymbol{r}_1^K + \frac{1}{6}\boldsymbol{r}_2^K + \frac{1}{6}\boldsymbol{r}_3^K, \qquad \boldsymbol{y}_1 = \frac{2}{3}\boldsymbol{r}_1^L + \frac{1}{6}\boldsymbol{r}_2^L + \frac{1}{6}\boldsymbol{r}_3^L, \tag{D.277}$$

$$\boldsymbol{x}_2 = \frac{1}{6}\boldsymbol{r}_1^K + \frac{2}{3}\boldsymbol{r}_2^K + \frac{1}{6}\boldsymbol{r}_3^K, \qquad \boldsymbol{y}_2 = \frac{1}{6}\boldsymbol{r}_1^L + \frac{2}{3}\boldsymbol{r}_2^L + \frac{1}{6}\boldsymbol{r}_3^L, \tag{D.278}$$

$$\boldsymbol{x}_3 = \frac{1}{6}\boldsymbol{r}_1^K + \frac{1}{6}\boldsymbol{r}_2^K + \frac{2}{3}\boldsymbol{r}_3^K, \qquad \boldsymbol{y}_3 = \frac{1}{6}\boldsymbol{r}_1^L + \frac{1}{6}\boldsymbol{r}_2^L + \frac{2}{3}\boldsymbol{r}_3^L. \tag{D.279}$$

When considering a function $\varphi : L \to \mathbb{C}$, the quadrature formula is given by

$$\int_L \left(\frac{t_d}{h_d^L}\right)^b \varphi(\boldsymbol{y})\,\mathrm{d}L(\boldsymbol{y}) \approx \frac{|L|}{3}\sum_{q=1}^{3}\left\{\frac{\left(\boldsymbol{y}_q - \boldsymbol{r}_d^L\right)\cdot\boldsymbol{\nu}_d^L}{h_d^L}\right\}^b \varphi(\boldsymbol{y}_q). \tag{D.280}$$

An equivalent formula is used when considering a function $\phi : K \to \mathbb{C}$, given by

$$\int_K \left(\frac{s_c}{h_c^K}\right)^a \phi(\boldsymbol{x})\,\mathrm{d}K(\boldsymbol{x}) \approx \frac{|K|}{3}\sum_{p=1}^{3}\left\{\frac{\left(\boldsymbol{x}_p - \boldsymbol{r}_c^K\right)\cdot\boldsymbol{\nu}_c^K}{h_c^K}\right\}^a \phi(\boldsymbol{x}_p). \tag{D.281}$$

The Gauss-Lobatto quadrature formula can be extended straightforwardly to a function of two variables, $\Phi : K \times L \to \mathbb{C}$, using both formulas shown above. Therefore

$$\int_K \int_L \left(\frac{s_c}{h_c^K}\right)^a \left(\frac{t_d}{h_d^L}\right)^b \Phi(\boldsymbol{x},\boldsymbol{y})\,\mathrm{d}L(\boldsymbol{y})\mathrm{d}K(\boldsymbol{x}) \approx \frac{|K|\,|L|}{9}\sum_{p=1}^{3}\sum_{q=1}^{3}\left\{\frac{\left(\boldsymbol{x}_p-\boldsymbol{r}_c^K\right)\cdot\boldsymbol{\nu}_c^K}{h_c^K}\right\}^a\left\{\frac{\left(\boldsymbol{y}_q-\boldsymbol{r}_d^L\right)\cdot\boldsymbol{\nu}_d^L}{h_d^L}\right\}^b\Phi(\boldsymbol{x}_p,\boldsymbol{y}_q). \quad \text{(D.282)}$$

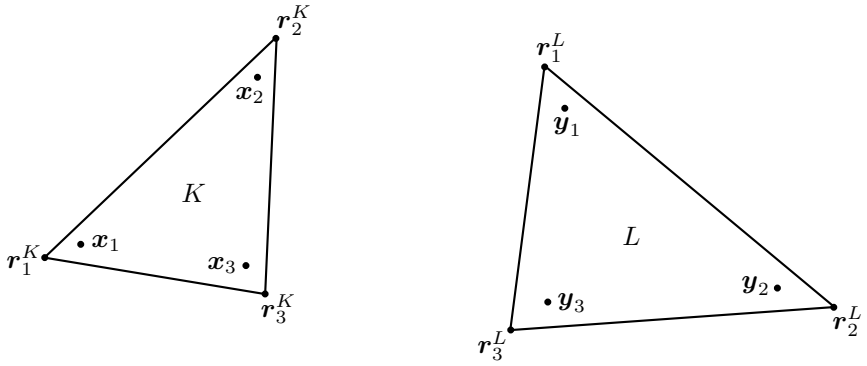

FIGURE D.12. Evaluation points for the three-point Gauss-Lobatto quadrature formulae.

b) Six-point Gauss-Lobatto quadrature formulae

For the six-point Gauss-Lobatto quadrature we consider respectively on the triangles K and L, as depicted in Figure D.13, the points

$$\boldsymbol{x}_1 = \alpha_1\boldsymbol{r}_1^K + \alpha_2\boldsymbol{r}_2^K + \alpha_2\boldsymbol{r}_3^K, \qquad \boldsymbol{y}_1 = \alpha_1\boldsymbol{r}_1^L + \alpha_2\boldsymbol{r}_2^L + \alpha_2\boldsymbol{r}_3^L, \quad \text{(D.283)}$$

$$\boldsymbol{x}_2 = \alpha_2\boldsymbol{r}_1^K + \alpha_1\boldsymbol{r}_2^K + \alpha_2\boldsymbol{r}_3^K, \qquad \boldsymbol{y}_2 = \alpha_2\boldsymbol{r}_1^L + \alpha_1\boldsymbol{r}_2^L + \alpha_2\boldsymbol{r}_3^L, \quad \text{(D.284)}$$

$$\boldsymbol{x}_3 = \alpha_2\boldsymbol{r}_1^K + \alpha_2\boldsymbol{r}_2^K + \alpha_1\boldsymbol{r}_3^K, \qquad \boldsymbol{y}_3 = \alpha_2\boldsymbol{r}_1^L + \alpha_2\boldsymbol{r}_2^L + \alpha_1\boldsymbol{r}_3^L, \quad \text{(D.285)}$$

$$\tilde{\boldsymbol{x}}_1 = \beta_1\boldsymbol{r}_1^K + \beta_2\boldsymbol{r}_2^K + \beta_2\boldsymbol{r}_3^K, \qquad \tilde{\boldsymbol{y}}_1 = \beta_1\boldsymbol{r}_1^L + \beta_2\boldsymbol{r}_2^L + \beta_2\boldsymbol{r}_3^L, \quad \text{(D.286)}$$

$$\tilde{\boldsymbol{x}}_2 = \beta_2\boldsymbol{r}_1^K + \beta_1\boldsymbol{r}_2^K + \beta_2\boldsymbol{r}_3^K, \qquad \tilde{\boldsymbol{y}}_2 = \beta_2\boldsymbol{r}_1^L + \beta_1\boldsymbol{r}_2^L + \beta_2\boldsymbol{r}_3^L, \quad \text{(D.287)}$$

$$\tilde{\boldsymbol{x}}_3 = \beta_2\boldsymbol{r}_1^K + \beta_2\boldsymbol{r}_2^K + \beta_1\boldsymbol{r}_3^K, \qquad \tilde{\boldsymbol{y}}_3 = \beta_2\boldsymbol{r}_1^L + \beta_2\boldsymbol{r}_2^L + \beta_1\boldsymbol{r}_3^L, \quad \text{(D.288)}$$

where

$$\alpha_1 = 0.816847572980459, \qquad \alpha_2 = 0.091576213509771, \quad \text{(D.289)}$$

$$\beta_1 = 0.108103018168070, \qquad \beta_2 = 0.445948490915965. \quad \text{(D.290)}$$

The weights are given by

$$\alpha_w = 0.109951743655322, \qquad \beta_w = 0.223381589678011. \quad \text{(D.291)}$$

When considering a function $\varphi : L \to \mathbb{C}$, the quadrature formula is given by

$$\int_L \left(\frac{t_d}{h_d^L}\right)^b \varphi(\boldsymbol{y})\,\mathrm{d}L(\boldsymbol{y}) \approx \alpha_w |L| \sum_{q=1}^{3} \left\{\frac{\left(\boldsymbol{y}_q - \boldsymbol{r}_d^L\right)\cdot \boldsymbol{\nu}_d^L}{h_d^L}\right\}^b \varphi(\boldsymbol{y}_q) + \beta_w |L| \sum_{q=1}^{3} \left\{\frac{\left(\tilde{\boldsymbol{y}}_q - \boldsymbol{r}_d^L\right)\cdot \boldsymbol{\nu}_d^L}{h_d^L}\right\}^b \varphi(\tilde{\boldsymbol{y}}_q). \tag{D.292}$$

An equivalent formula is used when considering a function $\phi : K \to \mathbb{C}$, given by

$$\int_K \left(\frac{s_c}{h_c^K}\right)^a \phi(\boldsymbol{x})\,\mathrm{d}K(\boldsymbol{x}) \approx \alpha_w |K| \sum_{p=1}^{3} \left\{\frac{\left(\boldsymbol{x}_p - \boldsymbol{r}_c^K\right)\cdot \boldsymbol{\nu}_c^K}{h_c^K}\right\}^a \phi(\boldsymbol{x}_p) + \beta_w |K| \sum_{p=1}^{3} \left\{\frac{\left(\tilde{\boldsymbol{x}}_p - \boldsymbol{r}_c^K\right)\cdot \boldsymbol{\nu}_c^K}{h_c^K}\right\}^a \phi(\tilde{\boldsymbol{x}}_p). \tag{D.293}$$

The Gauss-Lobatto quadrature formula can be extended straightforwardly to a function of two variables, $\Phi : K \times L \to \mathbb{C}$, using both formulas shown above. Therefore

$$\begin{aligned}
&\int_K \int_L \left(\frac{s_c}{h_c^K}\right)^a \left(\frac{t_d}{h_d^L}\right)^b \Phi(\boldsymbol{x},\boldsymbol{y})\,\mathrm{d}L(\boldsymbol{y})\mathrm{d}K(\boldsymbol{x}) \\
&\quad\approx \alpha_w^2 |K|\,|L| \sum_{p=1}^{3}\sum_{q=1}^{3} \left\{\frac{\left(\boldsymbol{x}_p - \boldsymbol{r}_c^K\right)\cdot \boldsymbol{\nu}_c^K}{h_c^K}\right\}^a \left\{\frac{\left(\boldsymbol{y}_q - \boldsymbol{r}_d^L\right)\cdot \boldsymbol{\nu}_d^L}{h_d^L}\right\}^b \Phi(\boldsymbol{x}_p,\boldsymbol{y}_q) \\
&\quad+ \beta_w^2 |K|\,|L| \sum_{p=1}^{3}\sum_{q=1}^{3} \left\{\frac{\left(\tilde{\boldsymbol{x}}_p - \boldsymbol{r}_c^K\right)\cdot \boldsymbol{\nu}_c^K}{h_c^K}\right\}^a \left\{\frac{\left(\tilde{\boldsymbol{y}}_q - \boldsymbol{r}_d^L\right)\cdot \boldsymbol{\nu}_d^L}{h_d^L}\right\}^b \Phi(\tilde{\boldsymbol{x}}_p,\tilde{\boldsymbol{y}}_q) \\
&\quad+ \alpha_w\beta_w |K|\,|L| \sum_{p=1}^{3}\sum_{q=1}^{3} \left\{\frac{\left(\tilde{\boldsymbol{x}}_p - \boldsymbol{r}_c^K\right)\cdot \boldsymbol{\nu}_c^K}{h_c^K}\right\}^a \left\{\frac{\left(\boldsymbol{y}_q - \boldsymbol{r}_d^L\right)\cdot \boldsymbol{\nu}_d^L}{h_d^L}\right\}^b \Phi(\tilde{\boldsymbol{x}}_p,\boldsymbol{y}_q) \\
&\quad+ \alpha_w\beta_w |K|\,|L| \sum_{p=1}^{3}\sum_{q=1}^{3} \left\{\frac{\left(\boldsymbol{x}_p - \boldsymbol{r}_c^K\right)\cdot \boldsymbol{\nu}_c^K}{h_c^K}\right\}^a \left\{\frac{\left(\tilde{\boldsymbol{y}}_q - \boldsymbol{r}_d^L\right)\cdot \boldsymbol{\nu}_d^L}{h_d^L}\right\}^b \Phi(\boldsymbol{x}_p,\tilde{\boldsymbol{y}}_q).
\end{aligned} \tag{D.294}$$

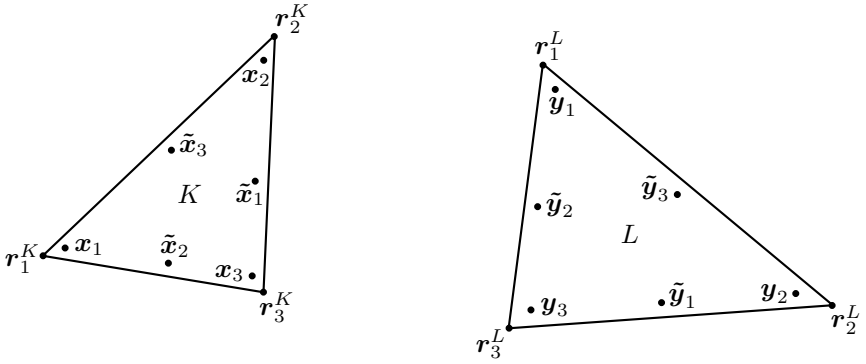

FIGURE D.13. Evaluation points for the six-point Gauss-Lobatto quadrature formulae.

c) Overall numerical integration

For the overall numerical integration we consider two different cases to achieve enough accuracy in the computations and to minimize the calculation time.

If the triangles K and L are not adjacent nor equal, then the integrals on K, (D.269) and (D.271), and the integrals on L, (D.270) and (D.272), are computed respectively using three-point Gauss-Lobatto quadrature formulae, i.e., (D.281) and (D.280), since in this case they are non-singular. Thus, in the whole, the integrals $ZA_{a,b}^{c,d}$ and $ZB_{a,b}^{c,d}$ are calculated employing (D.282).

On the other hand, if the triangles K and L have at least a common vertex, then the integrals on K are evaluated using the six-point Gauss-Lobatto quadrature formula (D.293), while the integrals on L, which become singular, are evaluated using the analytical formulae described next.

D.12.4 Analytical integration for the singular integrals

If the triangles K and L are close together, then the integrals (D.270) and (D.272) are calculated analytically, treating $\boldsymbol{x}$ as a given parameter. They are specifically given by

$$ZF_0^d(\boldsymbol{x}) = -\int_L \frac{1}{4\pi R}\,\mathrm{d}L(\boldsymbol{y}), \tag{D.295}$$

$$ZF_1^d(\boldsymbol{x}) = -\int_L \frac{t_d}{4\pi R\, h_d^L}\,\mathrm{d}L(\boldsymbol{y}), \tag{D.296}$$

and

$$ZG_0^d(\boldsymbol{x}) = \int_L \frac{\boldsymbol{R}\cdot\boldsymbol{n}_L}{4\pi R^3}\,\mathrm{d}L(\boldsymbol{y}), \tag{D.297}$$

$$ZG_1^d(\boldsymbol{x}) = \int_L t_d\,\frac{\boldsymbol{R}\cdot\boldsymbol{n}_L}{4\pi R^3\, h_d^L}\,\mathrm{d}L(\boldsymbol{y}). \tag{D.298}$$

a) Computation of $ZG_0^d(\boldsymbol{x})$

The integral (D.297) is closely related with Gauss's divergence theorem. If we consider an oriented surface differential element $\mathrm{d}\boldsymbol{\gamma} = \boldsymbol{n}_L \mathrm{d}L(\boldsymbol{y})$ seen from point $\boldsymbol{x}$, then we can express the solid angle differential element by (cf. Terrasse & Abboud 2006)

$$\mathrm{d}\Theta = \frac{\boldsymbol{R}}{R^3}\cdot\mathrm{d}\boldsymbol{\gamma} = \frac{\boldsymbol{R}\cdot\boldsymbol{n}_L}{R^3}\,\mathrm{d}L(\boldsymbol{y}) = 4\pi\frac{\partial G}{\partial n_{\boldsymbol{y}}}(\boldsymbol{x},\boldsymbol{y})\,\mathrm{d}L(\boldsymbol{y}). \tag{D.299}$$

Integrating over triangle L yields the solid angle Θ_L, as expressed in (D.245), namely

$$\Theta_L = \int_L \mathrm{d}\Theta \qquad (-2\pi \le \Theta_L \le 2\pi). \tag{D.300}$$

The solid angle Θ_L is positive when the vectors $\boldsymbol{R}$ and $\boldsymbol{n}_L$ point towards the same side of L. Thus integral (D.297) is obtained by integrating (D.299), which yields

$$ZG_0^d(\boldsymbol{x}) = \int_L \frac{\boldsymbol{R}\cdot\boldsymbol{n}_L}{4\pi R^3}\,\mathrm{d}L(\boldsymbol{y}) = \frac{\Theta_L}{4\pi}. \tag{D.301}$$

b) Computation of $ZF_0^d(\boldsymbol{x})$

For the integral (D.295) we consider before some vectorial identities and properties. We have that

$$\Delta R = \frac{1}{R^2}\frac{\partial}{\partial R}\left(R^2\frac{\partial R}{\partial R}\right) = \frac{2}{R}. \tag{D.302}$$

On the other hand, by using the relation (A.590) with the vector $R\,\boldsymbol{n}_L$ and performing afterwards a dot product with $\boldsymbol{n}_L$ yields

$$\Delta R = \frac{\partial^2 R}{\partial n^2} - \operatorname{curl}\operatorname{curl}(R\,\boldsymbol{n}_L)\cdot\boldsymbol{n}_L. \tag{D.303}$$

Since

$$\nabla R = \frac{\boldsymbol{R}}{R} \qquad \text{and} \qquad \nabla\nabla R = \frac{\mathbf{1}\otimes\mathbf{1}}{R} - \frac{\boldsymbol{R}\otimes\boldsymbol{R}}{R^3}, \tag{D.304}$$

therefore we obtain that

$$\frac{\partial R}{\partial n} = \frac{\boldsymbol{R}\cdot\boldsymbol{n}_L}{R} \qquad \text{and} \qquad \frac{\partial^2 R}{\partial n^2} = \frac{1}{R} - \frac{(\boldsymbol{R}\cdot\boldsymbol{n}_L)^2}{R^3}. \tag{D.305}$$

Hence, considering (D.302), (D.303), and (D.305), yields

$$\frac{1}{R} = -\frac{(\boldsymbol{R}\cdot\boldsymbol{n}_L)^2}{R^3} - \operatorname{curl}\operatorname{curl}(R\,\boldsymbol{n}_L)\cdot\boldsymbol{n}_L. \tag{D.306}$$

This way the integral (D.295) can be rewritten as

$$ZF_0^d(\boldsymbol{x}) = \int_L \frac{(\boldsymbol{R}\cdot\boldsymbol{n}_L)^2}{4\pi R^3}\,\mathrm{d}L(\boldsymbol{y}) + \frac{1}{4\pi}\int_L \operatorname{curl}\operatorname{curl}(R\,\boldsymbol{n}_L)\cdot\boldsymbol{n}_L\,\mathrm{d}L(\boldsymbol{y}). \tag{D.307}$$

Considering (D.244) and (D.301) for the first integral, and applying to the second one the curl theorem (A.617), yields

$$ZF_0^d(\boldsymbol{x}) = \frac{d_L\Theta_L}{4\pi} + \frac{1}{4\pi}\sum_{m=1}^{3}\int_{C_m^L} \operatorname{curl}(R\,\boldsymbol{n}_L)\cdot\boldsymbol{\tau}_m^L\,\mathrm{d}C(\boldsymbol{y}). \tag{D.308}$$

We have additionally, from (A.566), (A.589), and (D.234), that

$$\operatorname{curl}(R\,\boldsymbol{n}_L)\cdot\boldsymbol{\tau}_m^L = (\nabla R\times\boldsymbol{n}_L)\cdot\boldsymbol{\tau}_m^L = -\frac{\boldsymbol{R}}{R}\cdot(\boldsymbol{\tau}_m^L\times\boldsymbol{n}_L) = -\frac{\boldsymbol{R}\cdot\boldsymbol{\nu}_m^L}{R}. \tag{D.309}$$

Since $\boldsymbol{R}\cdot\boldsymbol{\nu}_m^L$ is constant on C_m^L, we can compute it as

$$\boldsymbol{R}\cdot\boldsymbol{\nu}_m^L = (\boldsymbol{R}_m^L + h_m^L\boldsymbol{\nu}_m^L)\cdot\boldsymbol{\nu}_m^L. \tag{D.310}$$

Hence (D.308) turns into

$$ZF_0^d(\boldsymbol{x}) = \frac{d_L\Theta_L}{4\pi} - \frac{1}{4\pi}\sum_{m=1}^{3}(\boldsymbol{R}_m^L + h_m^L\boldsymbol{\nu}_m^L)\cdot\boldsymbol{\nu}_m^L\int_{C_m^L}\frac{1}{R}\,\mathrm{d}C(\boldsymbol{y}), \tag{D.311}$$

where only the computation of the integral on C_m^L remains to be done.

c) Computation of $ZF_1^d(\boldsymbol{x})$

The integral (D.296) is somewhat simpler to treat. By replacing (D.241) inside this integral we obtain

$$\begin{aligned} ZF_1^d(\boldsymbol{x}) &= -\frac{1}{4\pi h_d^L}\int_L \frac{1}{R}\left(\boldsymbol{R}-\boldsymbol{R}_d^L\right)\cdot\boldsymbol{\nu}_d^L\,\mathrm{d}L(\boldsymbol{y}) \\ &= -\frac{1}{4\pi h_d^L}\int_L \frac{\boldsymbol{R}}{R}\cdot\boldsymbol{\nu}_d^L\,\mathrm{d}L(\boldsymbol{y}) - \frac{\boldsymbol{R}_d^L\cdot\boldsymbol{\nu}_d^L}{h_d^L}\,ZF_0^d(\boldsymbol{x}). \end{aligned} \tag{D.312}$$

It holds now that

$$\frac{\boldsymbol{R}}{R} = \nabla R = \frac{\partial R}{\partial n}\boldsymbol{n}_L + \nabla_L R, \tag{D.313}$$

where ∇_L denotes the surface gradient with respect to the parametrization of the plane of the triangle L. From (D.312) we obtain therefore

$$ZF_1^d(\boldsymbol{x}) = -\frac{\boldsymbol{\nu}_d^L}{4\pi h_d^L}\cdot\left(\int_L \frac{\partial R}{\partial n}\boldsymbol{n}_L\,\mathrm{d}L(\boldsymbol{y}) + \int_L \nabla_L R\,\mathrm{d}L(\boldsymbol{y})\right) - \frac{\boldsymbol{R}_d^L\cdot\boldsymbol{\nu}_d^L}{h_d^L}\,ZF_0^d(\boldsymbol{x}). \tag{D.314}$$

For the first integral in (D.314) we consider (D.244) and (D.305), which yields

$$\int_L \frac{\partial R}{\partial n}\boldsymbol{n}_L\,\mathrm{d}L(\boldsymbol{y}) = d_L\boldsymbol{n}_L\int_L \frac{1}{R}\,\mathrm{d}L(\boldsymbol{y}) = -4\pi d_L\boldsymbol{n}_L ZF_0^d(\boldsymbol{x}). \tag{D.315}$$

For the second integral in (D.314) we apply the Gauss-Green theorem (A.610) on the plane of the triangle L, which implies that

$$\int_L \nabla_L R\,\mathrm{d}L(\boldsymbol{y}) = \sum_{m=1}^{3}\boldsymbol{\nu}_m^L\int_{C_m^L} R\,\mathrm{d}C(\boldsymbol{y}). \tag{D.316}$$

Hence, by considering (D.315) and (D.316) in (D.314), we obtain

$$ZF_1^d(\boldsymbol{x}) = -\frac{\boldsymbol{\nu}_d^L}{4\pi h_d^L}\cdot\sum_{m=1}^{3}\boldsymbol{\nu}_m^L\int_{C_m^L} R\,\mathrm{d}C(\boldsymbol{y}) + \frac{\boldsymbol{\nu}_d^L}{h_d^L}\cdot\left(d_L\boldsymbol{n}_L - \boldsymbol{R}_d^L\right)ZF_0^d(\boldsymbol{x}), \tag{D.317}$$

where only the computation of the integral on C_m^L remains to be done.

d) Computation of $ZG_1^d(\boldsymbol{x})$

By replacing (D.241) and (D.244) inside the integral (D.298), we obtain

$$\begin{aligned} ZG_1^d(\boldsymbol{x}) &= \int_L \frac{\boldsymbol{R}\cdot\boldsymbol{n}_L}{4\pi R^3\,h_d^L}\left(\boldsymbol{R}-\boldsymbol{R}_d^L\right)\cdot\boldsymbol{\nu}_d^L\,\mathrm{d}L(\boldsymbol{y}) \\ &= \frac{d_L\boldsymbol{\nu}_d^L}{4\pi h_d^L}\cdot\int_L \frac{\boldsymbol{R}}{R^3}\,\mathrm{d}L(\boldsymbol{y}) - \frac{\boldsymbol{R}_d^L\cdot\boldsymbol{\nu}_d^L}{h_d^L}\,ZG_0^d(\boldsymbol{x}). \end{aligned} \tag{D.318}$$

Similarly as before, it holds that

$$-\frac{\boldsymbol{R}}{R^3} = \nabla\frac{1}{R} = \frac{\partial}{\partial n}\frac{1}{R}\,\boldsymbol{n}_L + \nabla_L\frac{1}{R}, \tag{D.319}$$

where ∇_L denotes again the surface gradient with respect to the parametrization of the plane of the triangle L. From (D.318) we obtain therefore

$$ZG_1^d(\boldsymbol{x}) = -\frac{d_L \boldsymbol{\nu}_d^L}{4\pi h_d^L} \cdot \left(\int_L \frac{\partial}{\partial n} \frac{1}{R} \, \boldsymbol{n}_L \, \mathrm{d}L(\boldsymbol{y}) + \int_L \nabla_L \frac{1}{R} \, \mathrm{d}L(\boldsymbol{y}) \right) - \frac{\boldsymbol{R}_d^L \cdot \boldsymbol{\nu}_d^L}{h_d^L} \, ZG_0^d(\boldsymbol{x}). \quad \text{(D.320)}$$

For the first integral in (D.320) we consider (D.301), which yields

$$\int_L \frac{\partial}{\partial n} \frac{1}{R} \, \boldsymbol{n}_L \, \mathrm{d}L(\boldsymbol{y}) = -\boldsymbol{n}_L \int_L \frac{\boldsymbol{R} \cdot \boldsymbol{n}_L}{R^3} \, \mathrm{d}L(\boldsymbol{y}) = -4\pi \boldsymbol{n}_L ZG_0^d(\boldsymbol{x}). \quad \text{(D.321)}$$

For the second integral in (D.320), as before, we apply the Gauss-Green theorem (A.610) on the plane of the triangle L, which implies that

$$\int_L \nabla_L \frac{1}{R} \, \mathrm{d}L(\boldsymbol{y}) = \sum_{m=1}^{3} \boldsymbol{\nu}_m^L \int_{C_m^L} \frac{1}{R} \, \mathrm{d}C(\boldsymbol{y}). \quad \text{(D.322)}$$

Hence, by considering (D.321) and (D.322) in (D.320), we obtain

$$ZG_1^d(\boldsymbol{x}) = -\frac{d_L \boldsymbol{\nu}_d^L}{4\pi h_d^L} \cdot \sum_{m=1}^{3} \boldsymbol{\nu}_m^L \int_{C_m^L} \frac{1}{R} \, \mathrm{d}C(\boldsymbol{y}) + \frac{\boldsymbol{\nu}_d^L}{h_d^L} \cdot \left(d_L \boldsymbol{n}_L - \boldsymbol{R}_d^L \right) ZG_0^d(\boldsymbol{x}), \quad \text{(D.323)}$$

where only the computation of the integral on C_m^L remains to be done.

e) Computation of the integrals on each edge C_m^L

The integrals on each edge C_m^L that remain to be computed are

$$\int_{C_m^L} \frac{1}{R} \, \mathrm{d}C(\boldsymbol{y}) \qquad \text{and} \qquad \int_{C_m^L} R \, \mathrm{d}C(\boldsymbol{y}). \quad \text{(D.324)}$$

To simplify the notation, we drop the indexes and denote the edge segment C_m^L just as C. Similarly, and as depicted in Figure D.14, we use also the notation:

- $|C|$ denotes the length of segment C.
- $\boldsymbol{R}_0, \boldsymbol{R}_1$ denote the endpoints of segment C, belonging to $\{\boldsymbol{R}_1^L, \boldsymbol{R}_2^L, \boldsymbol{R}_3^L\}$.
- $\boldsymbol{\tau}$ denotes the unit tangent of segment C, coinciding with $\boldsymbol{\tau}_m^L$.
- $\boldsymbol{\sigma}$ denotes the unit vector orthogonal to C that lies in the same plane as $\boldsymbol{x}$ and C.

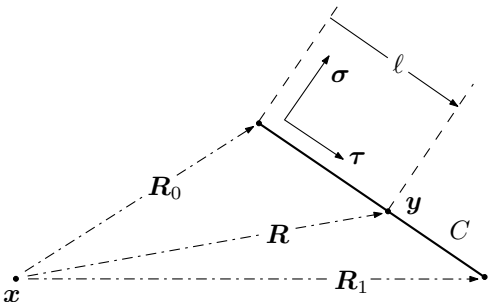

FIGURE D.14. Geometric characteristics for the calculation of the integrals on the edges.

We consider that the segment C is parametrically described by

$$\boldsymbol{R} = \boldsymbol{R}_0 + \ell\boldsymbol{\tau}, \qquad 0 \leq \ell \leq |C|, \tag{D.325}$$

and thus the parameter ℓ can be expressed as

$$\ell = (\boldsymbol{R} - \boldsymbol{R}_0) \cdot \boldsymbol{\tau} = |\boldsymbol{R} - \boldsymbol{R}_0|. \tag{D.326}$$

We have furthermore that

$$|C| = |\boldsymbol{R}_1 - \boldsymbol{R}_0| \qquad \text{and} \qquad \boldsymbol{R}_1 = \boldsymbol{R}_0 + |C|\boldsymbol{\tau}. \tag{D.327}$$

The unit vector $\boldsymbol{\sigma}$ that is orthogonal to C is given by

$$\boldsymbol{\sigma} = (\boldsymbol{R}_0 \times \boldsymbol{\tau}) \times \boldsymbol{\tau}. \tag{D.328}$$

Since we parametrized by ℓ, therefore all derivatives are taken with respect to this variable. It holds in particular that

$$RR' = \boldsymbol{R} \cdot \frac{\partial \boldsymbol{R}}{\partial \ell} = \boldsymbol{R} \cdot \boldsymbol{\tau}, \tag{D.329}$$

and hence

$$R(R + \boldsymbol{R} \cdot \boldsymbol{\tau})' = \boldsymbol{R} \cdot \boldsymbol{\tau} + R. \tag{D.330}$$

Consequently, by rearranging (D.330) we obtain

$$\frac{(R + \boldsymbol{R} \cdot \boldsymbol{\tau})'}{R + \boldsymbol{R} \cdot \boldsymbol{\tau}} = \frac{1}{R}. \tag{D.331}$$

Thus the first of the desired integrals in (D.324) is given by

$$\int_C \frac{1}{R}\,\mathrm{d}\ell = \ln\left(\frac{R_1 + \boldsymbol{R}_1 \cdot \boldsymbol{\tau}}{R_0 + \boldsymbol{R}_0 \cdot \boldsymbol{\tau}}\right). \tag{D.332}$$

We have also, from (D.329), that

$$\ell R' = \frac{\boldsymbol{R}}{R} \cdot (\ell\boldsymbol{\tau}) = R - \boldsymbol{R}_0 \cdot \frac{\boldsymbol{R}}{R}. \tag{D.333}$$

Expressing $\boldsymbol{R}_0, \boldsymbol{R}$ in terms of $\boldsymbol{\sigma}$ and $\boldsymbol{\tau}$ yields

$$\boldsymbol{R}_0 = (\boldsymbol{R}_0 \cdot \boldsymbol{\sigma})\boldsymbol{\sigma} + (\boldsymbol{R}_0 \cdot \boldsymbol{\tau})\boldsymbol{\tau}, \tag{D.334}$$

$$\boldsymbol{R} = (\boldsymbol{R}_0 \cdot \boldsymbol{\sigma})\boldsymbol{\sigma} + (\boldsymbol{R} \cdot \boldsymbol{\tau})\boldsymbol{\tau}, \tag{D.335}$$

$$\boldsymbol{R}_0 \cdot \boldsymbol{R} = (\boldsymbol{R}_0 \cdot \boldsymbol{\sigma})^2 + (\boldsymbol{R}_0 \cdot \boldsymbol{\tau})(\boldsymbol{R} \cdot \boldsymbol{\tau}), \tag{D.336}$$

and therefore, considering also (D.329), we obtain

$$\ell R' = R - \boldsymbol{R}_0 \cdot \frac{\boldsymbol{R}}{R} = R - \frac{1}{R}(\boldsymbol{R}_0 \cdot \boldsymbol{\sigma})^2 - (\boldsymbol{R}_0 \cdot \boldsymbol{\tau})R'. \tag{D.337}$$

By integrating we have that

$$\int_0^{|C|} \ell R'\,\mathrm{d}\ell = \int_C R\,\mathrm{d}\ell - (\boldsymbol{R}_0 \cdot \boldsymbol{\sigma})^2 \int_C \frac{1}{R}\,\mathrm{d}\ell - (\boldsymbol{R}_0 \cdot \boldsymbol{\tau})(R_1 - R_0). \tag{D.338}$$

An integration by parts on the left-hand side of (D.338) and a rearrangement of the terms yields finally the second of the desired integrals in (D.324), which is given by

$$\int_C R\,\mathrm{d}\ell = \frac{1}{2}\left(|C|R_1 + (\boldsymbol{R}_0 \cdot \boldsymbol{\sigma})^2 \int_C \frac{1}{R}\,\mathrm{d}\ell + (\boldsymbol{R}_0 \cdot \boldsymbol{\tau})(R_1 - R_0)\right). \tag{D.339}$$

We remark that from (D.336) we can express

$$(\boldsymbol{R}_0 \cdot \boldsymbol{\sigma})^2 = \boldsymbol{R}_0 \cdot \boldsymbol{R}_0 - (\boldsymbol{R}_0 \cdot \boldsymbol{\tau})^2. \tag{D.340}$$

f) Final computation of the singular integrals

In conclusion, the singular integrals (D.270) and (D.272) are computed using the formulae (D.301), (D.311), (D.317), and (D.323), where the integrals on the edges are calculated using (D.332) and (D.339).

It should be observed that $ZB_{a,b}^{c,d} = 0$ when the triangles coincide, i.e., when $K = L$, since in this case $d_L = 0$, and thus (D.301) and (D.323) become zero.

D.13 Benchmark problem

As benchmark problem we consider the exterior sphere problem (D.140), whose domain is shown in Figure D.4. The exact solution of this problem is stated in (D.161), and the idea is to retrieve it numerically with the integral equation techniques and the boundary element method described throughout this chapter.

For the computational implementation and the numerical resolution of the benchmark problem, we consider only the first integral equation of the extension-by-zero alternative (D.103), which is given in terms of boundary layer potentials by (D.176). The linear system (D.198) resulting from the discretization (D.196) of its variational formulation (D.183) is solved computationally with finite boundary elements of type $\mathbb{P}_1$ by using subroutines programmed in Fortran 90, by generating the mesh Γ^h of the boundary with the free software Gmsh 2.4, and by representing graphically the results in Matlab 7.5 (R2007b).

We consider a radius $R = 1$ and a constant impedance $Z = 0.8$. The discretized boundary surface Γ^h has $I = 702$ nodes, $T = 1400$ triangles, and a step $h = 0.2136$, being

$$h = \max_{1 \le j \le T} \operatorname{diam}(T_j). \tag{D.341}$$

As the known field without obstacle we take

$$u_W(r, \theta, \varphi) = \frac{\sin\theta\, e^{i\varphi} + \cos\theta}{r^2} = \frac{x_1 + i x_2 + x_3}{(x_1^2 + x_2^2 + x_3^2)^{3/2}}, \tag{D.342}$$

which implies that the impedance data function is given by

$$f_z(\theta, \varphi) = -\frac{\partial u_W}{\partial r}(R, \theta, \varphi) - Z u_W(R, \theta, \varphi) = -\frac{ZR - 2}{R^3}(\sin\theta\, e^{i\varphi} + \cos\theta). \tag{D.343}$$

The exact solution of the problem and its trace on the boundary are thus given by

$$u(\boldsymbol{x}) = -u_W(r, \theta, \varphi) = -\frac{\sin\theta\, e^{i\varphi} + \cos\theta}{r^2}, \tag{D.344}$$

$$\mu(\theta, \varphi) = -u_W(R, \theta, \varphi) = -\frac{\sin\theta\, e^{i\varphi} + \cos\theta}{R^2}. \tag{D.345}$$

The numerically calculated trace of the solution μ_h of the benchmark problem, which was computed by using the boundary element method, is depicted in Figure D.15. In the

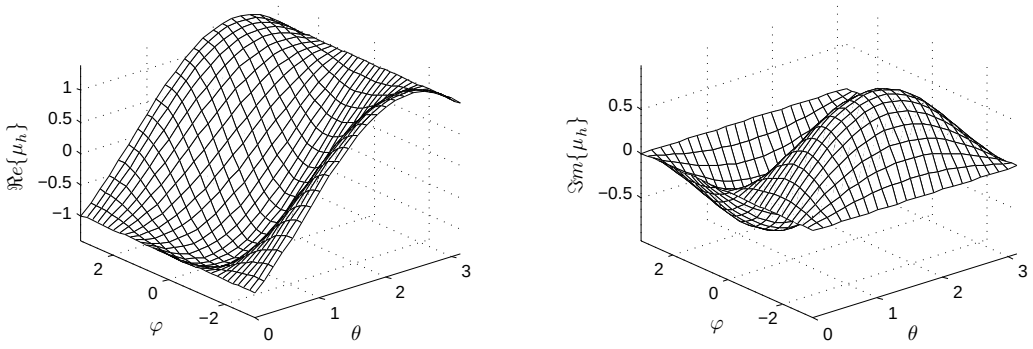

(a) Real part (b) Imaginary part

FIGURE D.15. Numerically computed trace of the solution μ_h.

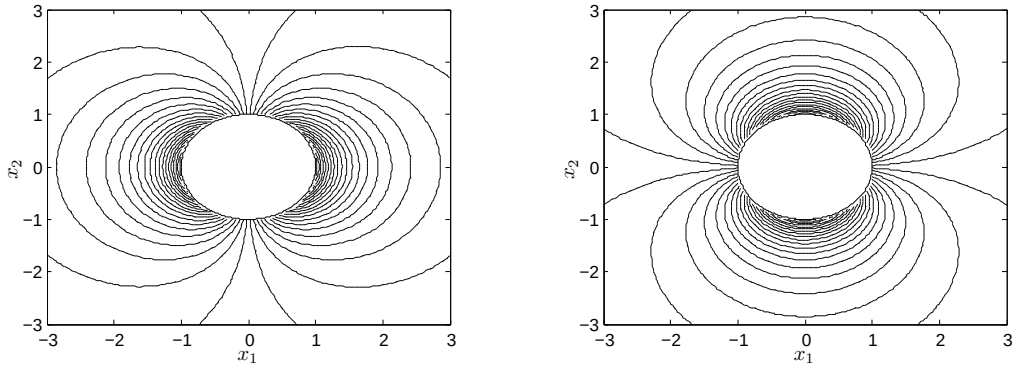

(a) Real part (b) Imaginary part

FIGURE D.16. Contour plot of the numerically computed solution u_h for $\theta = \pi/2$.

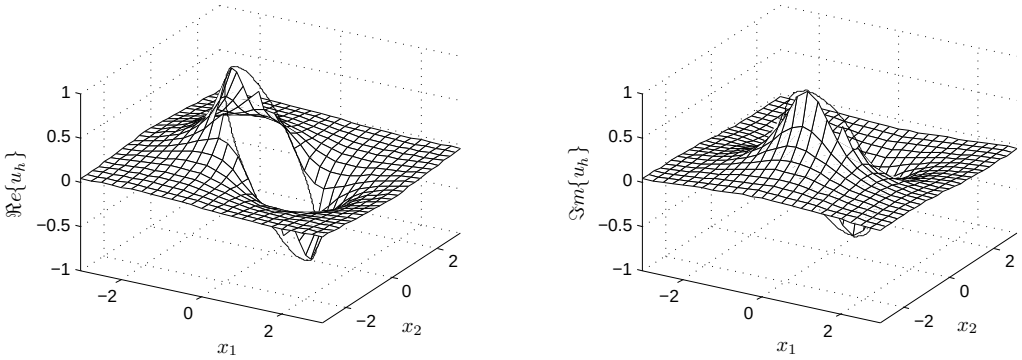

(a) Real part (b) Imaginary part

FIGURE D.17. Oblique view of the numerically computed solution u_h for $\theta = \pi/2$.

same manner, the numerical solution u_h is illustrated in Figures D.16 and D.17 for an angle $\theta = \pi/2$. It can be observed that the numerical solution is close to the exact one.

We define the relative error of the trace of the solution as

$$E_2(h, \Gamma^h) = \frac{\|\Pi_h \mu - \mu_h\|_{L^2(\Gamma^h)}}{\|\Pi_h \mu\|_{L^2(\Gamma^h)}}, \tag{D.346}$$

where $\Pi_h \mu$ denotes the Lagrange interpolating function of the exact solution's trace μ, i.e.,

$$\Pi_h \mu(\boldsymbol{x}) = \sum_{j=1}^{I} \mu(\boldsymbol{r}_j)\, \chi_j(\boldsymbol{x}) \quad \text{and} \quad \mu_h(\boldsymbol{x}) = \sum_{j=1}^{I} \mu_j\, \chi_j(\boldsymbol{x}) \quad \text{for } \boldsymbol{x} \in \Gamma^h. \tag{D.347}$$

It holds therefore that

$$\|\Pi_h \mu - \mu_h\|^2_{L^2(\Gamma^h)} = (\tilde{\boldsymbol{\mu}} - \boldsymbol{\mu})^* \boldsymbol{A}\, (\tilde{\boldsymbol{\mu}} - \boldsymbol{\mu}) \qquad \text{and} \qquad \|\Pi_h \mu\|^2_{L^2(\Gamma^h)} = \tilde{\boldsymbol{\mu}}^* \boldsymbol{A}\, \tilde{\boldsymbol{\mu}}, \tag{D.348}$$

where $\mu(\boldsymbol{r}_j)$ and μ_j are respectively the elements of vectors $\tilde{\boldsymbol{\mu}}$ and $\boldsymbol{\mu}$, for $1 \leq j \leq I$, and where the elements a_{ij} of the matrix $\boldsymbol{A}$ are specified in (D.256) and given by

$$a_{ij} = \langle \chi_j, \chi_i \rangle \qquad \text{for } 1 \leq i, j \leq I. \tag{D.349}$$

In our case, for a step $h = 0.2136$, we obtained a relative error of $E_2(h, \Gamma^h) = 0.01302$.

Similarly as for the trace, we define the relative error of the solution as

$$E_\infty(h, \Omega_L) = \frac{\|u - u_h\|_{L^\infty(\Omega_L)}}{\|u\|_{L^\infty(\Omega_L)}}, \tag{D.350}$$

being $\Omega_L = \{\boldsymbol{x} \in \Omega_e : \|\boldsymbol{x}\|_\infty < L\}$ for $L > 0$, and where

$$\|u - u_h\|_{L^\infty(\Omega_L)} = \max_{\boldsymbol{x} \in \Omega_L} |u(\boldsymbol{x}) - u_h(\boldsymbol{x})| \quad \text{and} \quad \|u\|_{L^\infty(\Omega_L)} = \max_{\boldsymbol{x} \in \Omega_L} |u(\boldsymbol{x})|. \tag{D.351}$$

We consider $L = 3$ and approximate Ω_L by a triangular finite element mesh of refinement h near the boundary. For $h = 0.2136$, the relative error that we obtained for the solution was $E_\infty(h, \Omega_L) = 0.02142$.

The results for different mesh refinements, i.e., for different numbers of triangles T, nodes I, and discretization steps h for Γ^h, are listed in Table D.1. These results are illustrated graphically in Figure D.18. It can be observed that the relative errors are approximately of order h^2.

TABLE D.1. Relative errors for different mesh refinements.

T	I	h	$E_2(h, \Gamma^h)$	$E_\infty(h, \Omega_L)$
32	18	1.0000	$5.112 \cdot 10^{-1}$	$5.162 \cdot 10^{-1}$
90	47	0.7071	$2.163 \cdot 10^{-1}$	$2.277 \cdot 10^{-1}$
336	170	0.4334	$5.664 \cdot 10^{-2}$	$7.218 \cdot 10^{-2}$
930	467	0.2419	$1.965 \cdot 10^{-2}$	$2.653 \cdot 10^{-2}$
1400	702	0.2136	$1.302 \cdot 10^{-2}$	$2.142 \cdot 10^{-2}$
2448	1226	0.1676	$6.995 \cdot 10^{-3}$	$1.086 \cdot 10^{-2}$

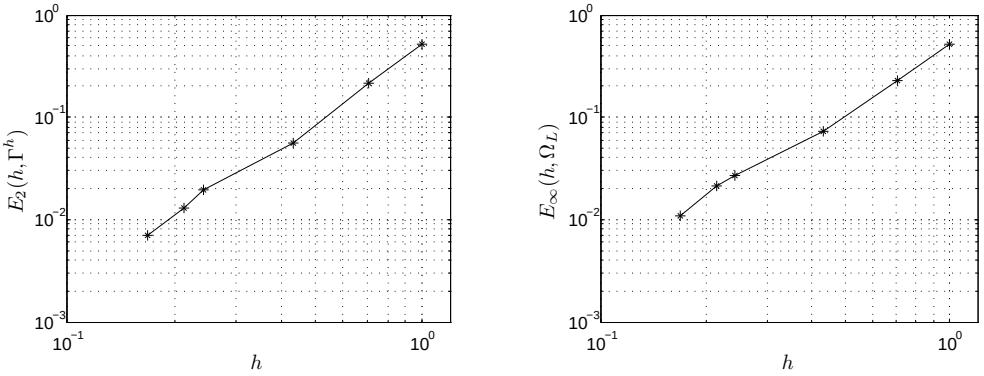

(a) Relative error $E_2(h, \Gamma^h)$ (b) Relative error $E_\infty(h, \Omega_L)$

FIGURE D.18. Logarithmic plots of the relative errors versus the discretization step.